Journal of Materials Chemistry B

Tunable Antibiotic Delivery from Gellan Hydrogels

Journal:	*Journal of Materials Chemistry B*
Manuscript ID	TB-ART-04-2018-000980.R1
Article Type:	Paper
Date Submitted by the Author:	12-Aug-2018
Complete List of Authors:	Shukla, Shashank; Brown University, School of Engineering Shukla, Anita; Brown University, School of Engineering

Journal of Materials Chemistry B

ARTICLE

Received 00th January 20xx,
Accepted 00th January 20xx
DOI: 10.1039/x0xx00000x
www.rsc.org/

Tunable Antibiotic Delivery from Gellan Hydrogels

Shashank Shukla[a] and Anita Shukla*[a]

Hydrogels are used extensively in wound management. Many wounds are highly susceptible to infection and hydrogels can provide localized antibacterial delivery to treat and prevent this infection. There are several key considerations in designing antibacterial hydrogels for wound therapy, including preserving activity of encapsulated antibacterial agents, controlling drug release timescales and concentrations, and having the ability to conform to various wound configurations. In this work, we have used gellan, a U.S. Food and Drug Administration approved food-additive, to develop antibiotic loaded hydrogels focusing on these criteria. These hydrogels were formed to exhibit a range of mechanical properties investigated using oscillatory rheology. We denoted hydrogels formed using 1% w/v gellan and 1 mM $CaCl_2$ "ointment" hydrogels and those formed using 4% w/v gellan and 7 mM $CaCl_2$ "sheet" hydrogels. Vancomcyin, a broad-spectrum antibiotic against gram-positive bacteria, was encapsulated in these hydrogels both directly and/or in graphitized carbon black nanoparticles (CNPs). We found that vancomycin released from both sheet and ointment hydrogels at therapeutically effective concentrations over 9 days with CNPs and 6 days without CNPs. Applying the Ritger-Peppas and Peppas-Sahlin semi-empirical drug release models to sheet hydrogels, we determined that Fickian diffusion dominates release while case II relaxation also has a small contribution. The sheet hydrogels had a larger overall release of drug (83.6 ± 1.6% compared to 67.0 ± 2.6% for ointments), which we attributed to larger swelling resulting from osmotic pressure differences between the hydrogel formulations and the release buffer. We also suggest that final drug release amounts are influenced by intermolecular interactions between vancomycin and gellan, which we observed via quartz crystal microbalance with dissipation monitoring. Lastly, we examined the potential for future *in vivo* translation. We demonstrated *in vitro* growth inhibition of *Staphylococcus aureus* (*S. aureus*) and methicillin-resistant *S. aureus* in the presence of these hydrogels, demonstrating that vancomycin activity is preserved upon encapsulation. We also showed that these hydrogels are non-toxic to important wound healing cells including fibroblasts and mesenchymal stem cells.

[a] *School of Engineering, Center for Biomedical Engineering, Institute for Molecular and Nanoscale Innovation, Brown University, Providence, RI, USA.*

*Corresponding author: anita_shukla@brown.edu

Electronic Supplementary Information (ESI) available: [Supporting information includes figures providing storage and loss moduli of non-drug loaded ointment and sheet hydrogels, equilibrium swelling ratio in various solutions, viscoelastic and mechanical properties of the hydrogel formulations, complete QCM-D data, vancomycin loading and release from CNPs, drug release from vancomycin loaded sheet and ointment hydrogels containing non-drug loaded CNPs, and hydrogel stability over time.]
See DOI: 10.1039/x0xx00000x

Keywords

Gellan, hydrogels, nanoparticles, drug delivery, vancomycin, antibiotics, wound infection, *Staphylococcus aureus*

Introduction

Hydrogels are among the most versatile biomaterials used in medical applications including drug delivery and tissue engineering. They are highly abundant in consumer healthcare products (e.g., contact lenses[1] and wound dressings[2-7]) and used widely in research involving injectable drug[8, 9] and growth factor[10, 11] delivery and cell encapsulation[12-14]. Several aspects of hydrogels also make them highly promising for the treatment of wounds. The hydrated polymeric network is capable of promoting wound healing[15], and hydrogels can generally be formulated to take on a variety of morphologies that can conform to various wounds[16]. Hydrogels can also be loaded with therapeutic factors that provide additional wound healing support[17], localized to the site of injury.

Wounds are highly susceptible to microbial infections, costing approximately 25 billion USD annually[18]. Approximately 2 million people in the U.S. are infected with antibiotic-resistant bacteria each year leading to 23,000 deaths[19]. With rising concerns over the development of antibiotic resistant bacteria and a lack of new antibiotics, hydrogels used in the treatment of wounds have the unique potential to locally treat possible infection. Localized delivery of antibiotics can lower or eliminate the need for systemic antibiotic administration, which can exacerbate resistance[20]. Common U.S. Food and Drug Administration (FDA)-approved polymers that have previously been used to formulate antibacterial hydrogels[21] include chitosan[9, 22, 23], alginate[24, 25], and poly(vinyl alcohol) (PVA)[4, 26, 27]. For some of these hydrogels, the polymeric network itself can exhibit antibacterial properties (e.g., chitosan), and in other cases, the hydrogel is loaded with antimicrobial therapeutics. The use of these polymers in formulating hydrogels that are potentially effective in treating infected wounds can be limited by the ease of tunability of mechanical properties, the stability of the material, and the potential effects of cross-linking conditions on encapsulated therapeutics. For example, PVA hydrogels are typically cross-linked with radiation, toxic chemicals, or repeated freeze-thaw cycles, all of which can have deleterious effects on small molecules incorporated during hydrogel formation[26]. On the other hand, alginate hydrogels formed via electrostatic interactions with added salts are relatively benign to encapsulated materials, but are known to have limited stability in biological conditions[2, 24].

In this work, we have developed antibiotic loaded hydrogels using gellan, a naturally produced heteropolysaccharide; these hydrogels can overcome many of the limitations of current antibacterial hydrogels. Gellan can yield physically cross-linked hydrogels that are mechanically robust in comparison to many other natural polysaccharides used in hydrogel formation[28, 29]. This enhanced stability is due to the dual gelation mechanism of gellan, which relies on both ionic interactions and helical aggregation[30]. Gellan polymer chains undergo a random coil to double-helix transition in aqueous conditions as the solution temperature is lowered to approximately 40°C; helical aggregation leads to water entrapment and hydrogel formation[29]. The addition of ions to the gelation solution aids in hydrogel formation by promoting charge shielding of the negatively charged carboxyl groups on the polymer backbone, which otherwise contribute to electrostatic repulsion of the polymer chains[29, 31]. Gellan hydrogel mechanical strength is particularly enhanced with the addition of divalent salts, such as calcium chloride ($CaCl_2$), at appropriate concentrations[32]. Gellan's interesting gelation properties have led to its use as an FDA-approved food additive and more recently in tissue engineering[33-36] and drug delivery research[37, 38]. Thus far, gellan has only been reported sparingly for antimicrobial applications primarily in the form of microspheres[39] or in ophthalmic drug delivery[40]. In biomaterials applications of gellan, hydrogels have typically been formulated at polymer and ion concentrations below 2% w/v and 5 mM salt, respectively[39, 40]. Here, we have focused on developing gellan hydrogels using polymer and ion concentrations both above and below these typical formulation conditions, in order to investigate the impact on hydrogel mechanical, antibacterial, and drug release properties.

The most common antimicrobial agents encapsulated into clinically utilized antimicrobial hydrogels include silver[41] and iodine[42]. However, these antimicrobials are known to be toxic to many important wound healing cells[43, 44]. Instead of these antimicrobials, we incorporated vancomycin, a broad-spectrum FDA-approved antibiotic, into gellan hydrogels. Vancomycin is highly effective against several gram-positive bacteria including *Staphylococcus aureus* and methicillin-resistant *S. aureus* (MRSA) at low minimum inhibitory concentrations (MICs)[45]. Although it has previously never been encapsulated in gellan-based hydrogels, vancomycin has been incorporated into other antibacterial biomaterials including multilayer films

and sponges[20, 46, 47], bone cement[48], and nanoparticles[49].

Here we have studied the effect of changing gellan polymer and ion concentration on hydrogel mechanical and swelling properties, along with vancomycin drug release kinetics. We found that while Fickian diffusion dominates vancomycin release from these hydrogels, case II relaxation transport also contributes. We also determined that drug release is influenced by vancomycin-gellan intermolecular interactions. In addition to direct incorporation of vancomycin during hydrogel formation, we explored the encapsulation of vancomycin into highly porous graphitized carbon black nanoparticles (CNPs), which were subsequently incorporated into the hydrogel during gelation. CNPs have been shown to have high molecular loading capacity. They can be formulated to have homogeneous size[50], and are also biocompatible. We hypothesizes that the surface properties[51] and high porosity of CNPs[52] would enable favorable interactions with vancomycin, allowing for drug loading The addition of vancomycin loaded CNPs to the hydrogel formulations increased drug release timescale and amount. Lastly, we demonstrated the *in vitro* efficacy of our vancomycin loaded gellan hydrogel formulations against *S. aureus* and MRSA, along with excellent cytocompatibility of these materials, providing support towards their eventual application in wound infection management.

Materials and Methods

Materials

Vancomycin hydrochloride from *Streptomyces orientalis*, graphitized carbon black nanoparticles (CNPs), $CaCl_2$ dihydrate ($CaCl_2 \cdot 2H_2O$), Dulbecco's phosphate buffered saline (1× PBS), sodium dodecyl sulfate (SDS), branched polyethyleneamine (BPEI), CCK8 Cell Counting Kit, high glucose Dulbecco's Modified Eagle's Medium (DMEM), bovine calf serum, and Gelzan™ CM Gelrite® gellan gum (deacetylated gellan, average molecular weight of 1 MDa) were purchased from Millipore Sigma (Billerica, MA). Hydrochloric acid (1 M), sodium hydroxide (1 M), BD BBL™ Sensi-Disc™ vancomycin susceptibility test discs, cation-adjusted Mueller Hinton II broth (CMHB), tryptic soy broth (TSB), BD Bacto™ dehydrated agar, penicillin-streptomycin solution (pen/strep), 60 mm petri dishes, and 8 mm disposable biopsy punches were obtained from Fisher Scientific (Waltham, MA). Human bone marrow derived mesenchymal stem cells (MSCs) and all related media were purchased from Lonza (Walkersville, MD). NIH 3T3 embryonic murine fibroblasts, *S. aureus* 25923, and MRSA MW2 strains were purchased from ATCC (Manassas, VA). Silica-coated quartz crystal microbalance crystals were purchased from Biolin Scientific (Västra Frölunda, Sweden). Milli-Q water (deionized water, 18.2 MΩ*cm, Millipore Sigma, Billerica, MA) was utilized in all experiments requiring water.

Materials Fabrication

Preparation of vancomycin loaded CNPs

CNPs were loaded with vancomycin by mixing 10 mg of vancomycin and 5 mg of CNPs in 2 mL of 1× PBS at 40 RPM for 10 minutes, 3 hours, or 24 hours at 23°C. Only CNPs loaded with vancomycin for 24 hours were incorporated into gellan hydrogels. To determine the amount of vancomycin loaded, vancomycin loaded CNPs were separated from free vancomycin in solution, by centrifugation at 6000 RPM for 20 minutes. The vancomycin concentration in the supernatant was quantified by examining the absorbance of this solution at a wavelength of 281 nm wavelength using a Cytation3 Plate Reader (BioTek®) and comparing with vancomycin standards. This free vancomycin mass was subtracted from the initial vancomycin mass available for loading to yield the total vancomycin loaded.

Hydrogel formulation

To formulate hydrogels, gellan was first mixed with deionized water and heated to approximately 120°C. Vancomycin loaded CNPs (formulated as described in Materials Fabrication: Preparation of vancomycin loaded CNPs) were dried at 50°C. Dried vancomycin loaded CNPs were mixed with $CaCl_2$ and vancomycin in a total volume of 5 mL of deionized water. This mixture was immediately added to 45 mL of the gellan solution (cooled to approximately 50°C) and mixed thoroughly. The final concentrations of vancomycin in vancomycin loaded CNPs and free vancomycin in the gellan solution were 0.2 mg/mL and 0.4 mg/mL, respectively. The final gellan concentration was either 1 or 4% w/v, while the final $CaCl_2$ concentration was 1 or 7 mM. The gellan, ion, and drug mixture (30 mL) was poured into 60 mm petri dishes. The mixture was allowed to cool at 23°C, allowing the hydrogels to set. Cylindrical hydrogels were punched out of these large hydrogels using biopsy punches, yielding hydrogel cylinders 8 mm in diameter and 13.3 mm in height (volume: 0.67 mL). These hydrogels were stored at 4°C prior to use. The final vancomycin and CNP content of the cylindrical hydrogels is listed in Table 1. We also formulated hydrogels with free vancomycin (267 μg) and empty CNPs (70 μg), as well as hydrogels with vancomycin loaded CNPs (70 μg CNPs containing 133 μg vancomcyin) and no free vancomycin.

Table 1: Composition of gellan hydrogels[a]

Hydrogel description	Gellan concentration (% w/v)	$CaCl_2$ concentration (mM)	Free vancomycin per gel (μg)	CNPs per gel (μg)	Vancomycin loaded in CNPs (μg)[b]	Total vancomycin per gel (μg)
ointment	1	1	0	0	0	0
ointment + vancomycin	1	1	400	0	0	400
ointment composite	1	1	267	70	133	400
sheet	4	7	0	0	0	0
sheet + vancomycin	4	7	400	0	0	400
sheet composite	4	7	267	70	133	400

[a]Each hydrogel was a cylinder with 8 mm diameter and 13.3 mm length (0.67 mL volume).

[b]The amount of vancomcyin contributed from the vancomycin loaded CNPs was calculated by determining the mass of vancomycin loaded per mass of CNPs during complex formation as described in "Materials fabrication: Preparation of vancomycin loaded CNPs."

Journal of Materials Chemistry B

ARTICLE

To confirm that vancomycin was homogeneously distributed in our hydrogel structure, (which would yield 400 µg per each cylindrical 0.67 mL hydrogel), we analyzed the vancomycin content of non-CNP loaded hydrogel samples from various locations within our larger 60 mm petri dish hydrogel. Several hydrogel cylinders were taken randomly and melted at 60°C and diluted in DI water (1:5 v/v). The amount of vancomycin in these hydrogels was determined by examining the absorbance of these solutions at a 281 nm wavelength, as described earlier (see Materials fabrication: Preparation of vancomycin loaded CNPs).

Characterization of hydrogel physical properties

Hydrogel morphological analysis and mechanical properties analysis

Macroscale morphology of all hydrogel samples was examined with digital camera imaging using a Canon PowerShot S110. The microscale morphology of these hydrogels was examined using scanning electron microscopy (Zeiss LEO 1530 VP ultra-high resolution field emission SEM). The hydrogel samples were lyophilized, fractured, and sputter coated with gold prior to imaging on SEM at 10 kV.

Oscillatory rheology was used to examine viscoelastic properties[53] for hydrogels formulated with and without vancomycin loaded CNPs at 23°C using a TA Advanced Rheometer 2000 (TA Instruments). Applying 10% strain, a frequency sweep was carried out over an angular frequency range of 10 Hz to 600 Hz. The storage (G') and loss (G") moduli of the hydrogels were determined over this angular frequency range. Viscosity as a function of shear rate was also investigated for ointment hydrogels (with and without vancomycin and vancomycin loaded CNPs). A shear rate ramp from 0.1 to 10 s^{-1} was carried out at 37°C and viscosity was determined.

The Young's moduli of 4% gellan, 7 mM $CaCl_2$ hydrogels formulated with and without vancomycin and vancomycin loaded CNPs were evaluated through compression testing using a Bose Enduratec® ELF 3200 (TA Instruments) equipped with a top indenter and bottom parallel plate at 23°C. The specimens were preloaded with a 0.5 g load cell. The force applied was measured while the specimen was deformed to 10% of the initial sample thickness upon preloading. An engineering stress (σ) versus strain (ε) curve was developed from these measurements, and the Young's modulus was determined as the slope of the linear region.

Hydrogel swelling properties

The swelling capabilities of all hydrogel samples were examined in four different incubation solutions at 37°C: deionized water, 1× PBS, 1 mM $CaCl_2$ in deionized water, and 7 mM $CaCl_2$ in deionized water. A rehydration ratio (Figure S1A) representing the ability of the hydrogel to regain its original post-fabrication hydrated mass following complete dehydration and subsequent exposure to the incubation solutions was evaluated. To examine the rehydration ratio, hydrogels were weighed upon fabrication ($Mass_0$). These hydrogels were then lyophilized leading to complete dehydration. The lyophilized samples were submerged in 2 mL of the respective swelling solutions for 48 hours. The new reswollen hydrogel mass ($Mass_{t=48\ hours}$) was recorded. The rehydration ratio was calculated using eq (1).

$$Rehydration\ ratio = \frac{Mass_{t=48\ hours}}{Mass_0} \quad (1)$$

An equilibrium swelling ratio (Q_s) (Figure S1B) was also evaluated using eq (2)[54, 55].

$$Q_s = \frac{(W_s - W_d)}{W_d} \quad (2)$$

Here, W_s is the wet mass of the hydrogel after incubation in the swelling solutions for 48 hours post-fabrication. W_d is the dry mass of these hydrogels obtained via lyophilization following this swelling period. Swollen – initial mass of the hydrogels was also quantified by subtracting the initial post fabrication ointment and sheet hydrogel mass (W_i) from their respective swollen mass (W_s) following 48 hours of incubation in solution.

Hydrogel stability

Stability of hydrogels with and without CNPs was examined by quantifying change in hydrated hydrogel mass over time in both deionized water and 1× PBS at 4°C, 20°C, and 37°C over 25 and 77 days, respectively. Hydrogels were weighed upon fabrication ($Mass_0$), placed in 2 mL of the desired incubation solution, and at various times they were removed and weighed to assess the hydrated mass ($Mass_t$). Change in hydrogel mass at these time points compared to the initial mass was quantified using eq (3).

$$Percent\ change\ in\ hydrogel\ mass\ (\%) = \frac{Mass_t - Mass_0}{Mass_0} \times 100\% \quad (3)$$

Examining vancomycin release

Vancomycin release from hydrogels and CNPs

Gellan hydrogels were submerged in 2 mL of 1× PBS (pH 7.4) with no agitation at 37°C to monitor drug release. The 1× PBS solution was carefully collected and completely

replaced with fresh 1× PBS every 24 hours. The vancomycin content in the release solution was quantified by measuring absorbance at 281 nm, as described earlier (see Materials fabrication: Preparation of vancomycin loaded CNPs). The release study was continued until vancomycin concentration was below the absorbance detection limit (approximately 1 µg/mL). For drug release modeling studies examining only the first 60% of release, a release study was conducted for 48 hours where the 1× PBS solution was replaced at 24 hours. During this study, 100 µL of the release solution was carefully removed every 6 hours and vancomycin concentration was quantified as previously described.

Release of vancomycin from vancomycin loaded CNPs was also examined. The CNPs (20 mg) were submerged in 1 mL of 1× PBS (pH 7.4) at 37°C to monitor drug release. Every 24 hours, the CNPs were centrifuged at 1500 RPM for 5 minutes, leading to CNP pellet formation. The 1× PBS solution was carefully removed and replaced with fresh 1× PBS. The vancomycin content in the 1× PBS collected was quantified by measuring absorbance at 281 nm. This release study was continued until vancomycin release was below detectable concentrations (approximately 1 µg/mL).

Studying vancomycin-gellan interactions

Quartz crystal microbalance with dissipation monitoring (QCM-D) was used to analyze potential molecular interactions between gellan and vancomycin using a QCM-D E4 system (Biolin Scientific). QCM-D experiments were conducted in deionized water at 25°C and frequency and dissipation changes were monitored over time. Silica-coated QCM-D substrates were utilized in these experiments. Prior to use in QCM-D experiments, the substrates were cleaned as previously reported[56]. Briefly, the silica substrates were cleaned with deionized water, 2% w/v SDS, and deionized water again followed by drying with N_2 and UV/ozone treatment with a UV/ozone ProCleaner (Bioforce Nanosciences)[56]. A flow rate of 150 μL/min was used for gellan, deionized water, and BPEI, and a flow rate of 50 μL/min was used for vancomycin. An initial priming layer of BPEI was flowed over the substrate at a concentration of 1 mg/mL for approximately 10 minutes followed by a deionized water rinse for 10 minutes. Next, gellan at a concentration of 1 mg/mL was flowed; once the change in frequency plateaued a deionized water rinse was introduced. Vancomycin was then introduced at a concentration of 0.25 mg/mL followed by a final deionized water rinse.

Hydrogel antibacterial efficacy

Inhibition of *S. aureus and* MRSA growth by hydrogels and hydrogel drug release samples was examined using modified Kirby-Bauer[57, 58] and microdilution assays[59], respectively. For the modified Kirby-Bauer assays, *S. aureus* or MRSA in the exponential growth phase at a concentration of 10^8 colony forming units (CFU)/mL was evenly applied over a CMHB-agar surface. Composite hydrogels (i.e., hydrogels with free vancomycin and vancomycin loaded CNPs) were placed on the bacteria coated plates along with non-drug loaded hydrogels as negative controls and 30 μg vancomycin susceptibility discs as positive controls. Following 18 hours of incubation at 37°C, the agar plates were examined for zones of inhibition surrounding the test samples using digital camera imaging with a Canon PowerShot S110.

The efficacy of hydrogel drug release samples in 1× PBS was examined using microdilution assays, as previously described[20, 46, 47]. These samples were added in triplicate upon filtration through a 0.2 μm filter into 96 well clear bottom plates. Samples were diluted in 2× CMHB to yield a final concentration of 1× CMHB. The samples were then serially diluted 1:2 in 1× CMHB. As a control, sterile 1× PBS without any vancomycin was included and similarly diluted in CMHB. *S. aureus* or MRSA in its exponential growth phase was added to these diluted samples at a final concentration of 10^5 CFU/mL, along with positive controls of 1× PBS without vancomycin. Negative controls of 1× PBS did not contain any bacteria. Controls of non-hydrogel incorporated vancomycin at a known concentration were also examined. Well plates were incubated at 37°C for 18 hours with shaking at 90 RPM. Optical density (OD) of all wells in these plates was measured at 600 nm using a Cytation3 Plate Reader (BioTek®). The normalized bacteria density was calculated using eq (4)[46].

$$Normalized\ Bacteria\ Density = \frac{OD_{600,sample} - OD_{600,negative\ control}}{OD_{600,positive\ control} - OD_{600,negative\ control}} \quad (4)$$

***In vitro* hydrogel biocompatibility**

Hydrogel biocompatibility was investigated by examining viability of MSCs and NIH 3T3 embryonic murine fibroblasts upon exposure to hydrogel-incubated culture media. Hydrogels (gellan, gellan + vancomycin, gellan + CNPs, and composite, for both sheet and ointment formulations) and vancomycin (400 µg) were incubated in 1 mL of the appropriate cell culture media (Lonza growth media for the MSCs and DMEM with 10% calf bovine serum and 1% pen/strep for the NIH 3T3 cells) for 1 and 9 days. Cells (passage 5 or 6 for MSCs) were seeded at a density of 10,000 cells per cm^2 in a 96 well polystyrene tissue culture plate and incubated at 37°C and 5% CO_2 in 100 µL of the appropriate cell culture media for 24 hours. All test samples were sterile filtered using 0.2 µm filters and the media on the plated cells was replaced with 100 µL of the test samples. Positive controls of cells cultured in untreated media and negative controls of untreated media containing no cells were included. After 18 hours of exposure to sample media, a CCK8 viability assay was performed. Media was aspirated from the wells and 150 µL of CCK8 reagent was added. Cell viability was quantified by measuring the absorbance of the wells at 450 nm using a Cytation3 Plate Reader (BioTek®) following 2 hours of incubation at 37°C. Cell viability was calculated as follows:

$$Normalized\ cell\ viability = \frac{(Abs_{450,sample} - Abs_{450,negative\ control})}{(Abs_{450,positive\ control} - Abs_{450,negative\ control})} \quad (5)$$

Statistical analysis and modeling

All experiments were repeated at least three times and at least three individual samples were included in each experimental repeat. Drug release modeling was evaluated using GraphPad Prism 7. Statistical significance was calculated using GraphPad Prism with either a two-tailed t-test or one- or two-way analysis of variance (ANOVA) with Tukey's post-hoc analysis, as appropriate. Data was considered statistically significant for $p < 0.05$.

Results and Discussion

Gellan hydrogel fabrication and characterization

Gellan hydrogels have previously been formulated using covalent modifications[60] and ion-mediated crosslinking[61]. In this work, we focused on ionotropic gelation only, which has a greater potential to preserve the activity of a variety of encapsulated species. Previous studies involving gellan hydrogels for drug delivery have typically utilized gellan concentrations lower than 2% w/v, monovalent salts, or concentrations of divalent salts below 5 mM[62-67]. Here we have utilized gellan and divalent salt ($CaCl_2$) concentrations that span beyond this range in order to investigate the impact of these factors on hydrogel gelation and drug release properties. Figure 1A and 1B show the deacetylated gellan repeat unit structure

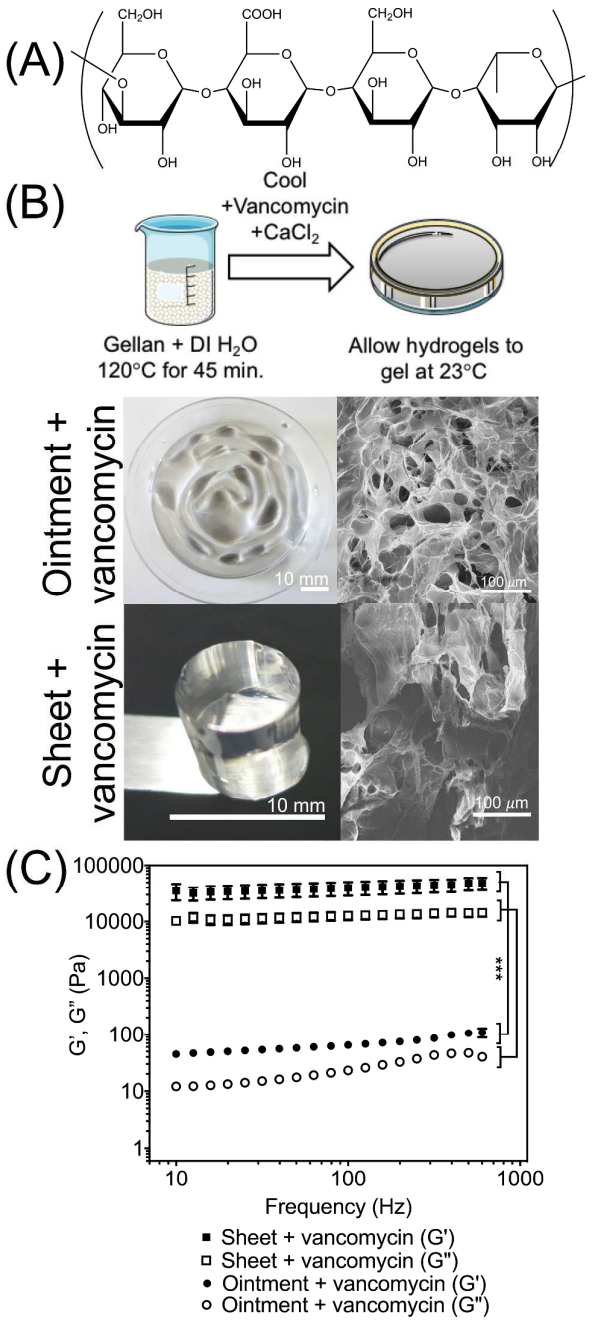

Figure 1: Vancomycin loaded gellan hydrogel gelation and mechanical properties. (A) Deacetylated gellan repeat unit chemical structure. (B) Drug loaded hydrogel formulation process. Gellan and deionized water are heated to 120°C to fully dissolve the gellan polymer, and then cooled to ~ 50°C, followed by the addition of vancomycin and $CaCl_2$. The hydrogels are then further cooled and allowed to set at at 23°C. Representative digital images of vancomycin loaded ointment (1% w/v gellan, 1 mM $CaCl_2$) and sheet (4% w/v gellan, 7 mM $CaCl_2$) hydrogels are shown along with SEM images of freeze-dried and fractured hydrogels. (C) Storage (G') and loss (G") moduli of vancomycin loaded ointment and sheet hydrogels over a frequency sweep of 10 to 600 Hz. Data are shown as mean ± standard deviation; significance was calculated using a two-tailed t-test indicating that ***$p < 0.001$ for G' and G" between sheet and ointment hydrogels ($n = 5$).

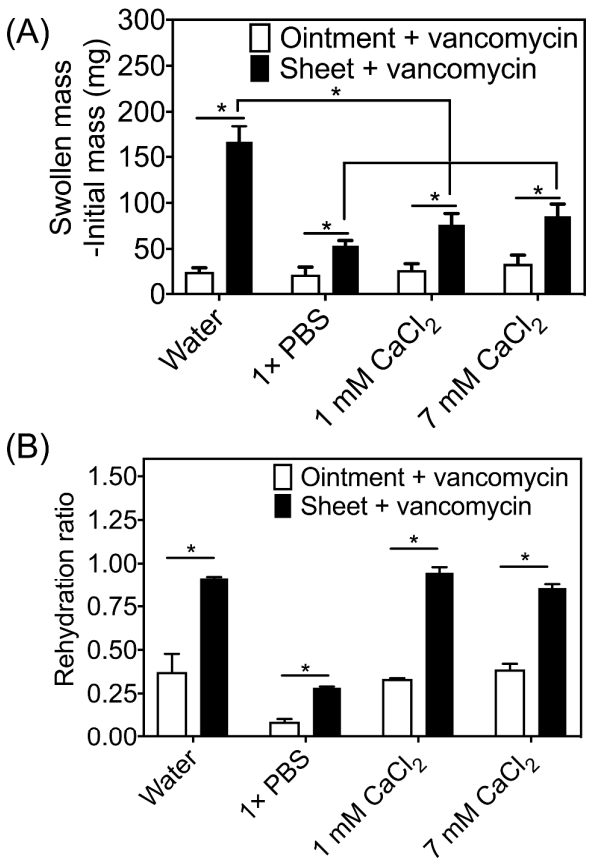

Figure 2: Vancomycin loaded gellan hydrogel swelling analysis in deionized water, 1× PBS, and 1 mM and 7 mM $CaCl_2$ solutions at 37°C. (A) Mass uptake of vancomycin loaded ointment and sheet hydrogels incubated in swelling solutions represented as a mass difference between 48 hour-swollen hydrogels and their initial post-hydrogel fabrication mass. (B) Rehydration ratio of vancomycin loaded ointment and sheet hydrogels incubated in the respective swelling solutions following complete dehydration of the hydrogels. Data are shown as mean ± standard deviation. Significance was calculated using a two-tailed t-test (*$p < 0.05$ between the groups indicated ($n = 3$).

and summarize the gellan hydrogel fabrication process utilized, respectively. Using 1% w/v gellan with 1 mM $CaCl_2$, we formulated hydrogels, which we will refer to as "ointment" hydrogels, while 4% w/v gellan with 7 mM $CaCl_2$ resulted in more solid hydrogels, which we will refer to as "sheet" hydrogels. Vancomycin addition during gelation at a relatively high concentration (0.6 mg/mL), did not hinder hydrogel formation. The ointment formulation was readily extruded through a 25.5 gauge needle, a typical needle gauge utilized in subcutaneous injection[68], supporting its potential for use as an injectable hydrogel. Viscosity measurements of the ointment hydrogels from a shear rate of 0.1-10 s^{-1} indicated shear thinning behavior (Figure S2), a common phenomenon observed for injectable hydrogels[69, 70]. The sheet hydrogel, in contrast, was not as readily deformed, due to the higher ion and polymer concentration. Representative digital images of vancomycin loaded ointment sheet hydrogels are shown in Figure 1B. Cross-sectional SEM images of freeze-dried ointment and sheet hydrogels displayed heterogeneous porosity, with more defined pores in the ointment formulations compared to the sheet (Figure 1B).

Oscillatory rheology was used to evaluate ointment and sheet hydrogel mechanical properties, as shown in Figure 1C. We observed an approximate 3 orders of magnitude difference in the storage (G') and loss (G") moduli values between the ointment and the sheet hydrogels. No difference was observed for G' and G'' of hydrogels formulated with (Figure 1C) and without vancomycin (Figure S3). The Young's modulus of vancomycin loaded sheet hydrogels was measurable via compression testing and determined to be 135 ± 48 kPa. Similar Young's moduli, G', and G" values have been observed for physically crosslinked gellan hydrogels used in tissue engineering[33, 71].

Vancomycin loaded ointment and sheet hydrogel swelling properties were examined in solutions of 1× PBS, $CaCl_2$ in deionized water, and deionized water (Figure 2), to examine the effects of salt content on swelling. Swelling in $CaCl_2$ solutions was examined at both a low and high $CaCl_2$ concentration using the same $CaCl_2$ molarities used in hydrogel fabrication, 1 mM $CaCl_2$ and 7 mM $CaCl_2$. Here, deionized water was utilized as a condition lacking dissolved salts. 1× PBS was used to mimic the ion content of biological fluids[72, 73], and the $CaCl_2$ solutions were used to investigate the effect of a single salt at different concentrations in solution. Figure 2A shows the difference between the swollen mass of hydrogels following 48 hours of incubation with these solutions and the initial post-fabrication ointment and sheet hydrogel mass. We observed a significantly greater mass difference for sheet versus ointment hydrogels in all swelling solutions. For polyelectrolyte hydrogels, free cations remain in the hydrogel network to neutralize the fixed charges on the polymer backbone when the hydrogel is exposed to deionized water, setting up a large osmotic pressure differential and promoting water infiltration and swelling. This effect is more pronounced in the sheet hydrogels than the ointment due to the larger polymer and ion concentration used in forming these gels. For the sheet hydrogels, the mass uptake during swelling was significantly lower in the salt solutions (1 and 7 mM $CaCl_2$ and 1× PBS) compared to the deionized water as shown in Figure 2A. In higher salt solutions, the ions will diffuse into the hydrogel network reducing the concentration difference between ions inside the hydrogel and outside, thus lowering the driving force for swelling[74]. An equilibrium swelling ratio (Q_s) (i.e., the ratio of the hydration mass to the dry matrix mass[33, 75, 76]) was also determined for the vancomycin loaded sheet and ointment hydrogels as shown in Figure S3. Overall, we observed that Q_s was significantly greater for the ointment hydrogels than the sheet hydrogels in any given swelling solution. Note, normalization by the significantly larger dry mass of the sheet hydrogels as compared to the ointment hydrogels in the calculation of Q_s results in a larger Q_s for the ointment versus sheet

hydrogels in all conditions tested. For both sheet and ointment hydrogels, Q_s was significantly lower in the salt solutions (1 and 7 mM $CaCl_2$ and 1× PBS) compared to deionized water, as expected. The difference between swollen and initial sheet hydrogel mass along with Q_s for both sheet and ointment was lowest for hydrogels incubated in 1× PBS, which can be attributed to the greater total salt concentration in 1× PBS compared to the other incubation solutions, reducing the osmotic pressure difference between the hydrogel and the incubation solution.

The rehydration ratio following lyophilization of the hydrogels was also investigated. Figure 2B shows the ratio of the hydrogel mass regained after rehydrating in 1× PBS, $CaCl_2$ in deionized water, and deionized water compared with the original hydrogel mass before dehydration. Larger rehydration ratios were observed for sheet versus ointment hydrogels in all of the solutions, with sheet hydrogels in deionized water and $CaCl_2$ returning close to their original pre-drying mass (91.5 ± 0.8% rehydration in water; 94.8 ± 3.2% rehydration in 1 mM $CaCl_2$; 85.5 ± 2.2% rehydration in 7 mM $CaCl_2$). This difference in rehydration ratio between the sheet and ointment hydrogels is likely due to the larger gellan and $CaCl_2$ concentrations used to formulate sheet hydrogels, leading to a larger osmotic pressure difference between the dry hydrogel network and the surrounding solution during rehydration[77]. We also observed that the rehydration ratio was lowest for 1× PBS, similarly to Q_s and the mass difference between swollen and post-fabrication hydrogel mass.

Vancomycin release from gellan hydrogels

Once the morphology, mechanical, and swelling properties of vancomycin loaded hydrogels were investigated, drug release was examined in 1× PBS at 37°C. First, we confirmed that vancomycin loading was consistent between individual hydrogel samples at 400 μg for both sheet and ointment hydrogels. Melting hydrogel cylinders and examining vancomycin content, we observed that there was 401 ± 3.9 μg and 398 ± 3.5 μg of vancomycin loaded in sheet and ointment hydrogels, suggesting homogeneous drug loading. Figure 3A shows cumulative vancomycin release over time as well as percentage of vancomycin released normalized to the total vancomycin loaded in the hydrogel. Both ointment and sheet hydrogels released vancomycin over at least 6 days. Following 6 days, additional vancomycin release was not detected, indicating that any drug released following 6 days was at concentrations below 1 μg/mL (this concentration is approximately equivalent to the MIC of vancomycin against most S. aureus and MRSA strains46 and was at the lower limit of our instrument detection range for vancomycin). Sheet hydrogels released 50.7 ± 1.2% of the total vancomycin loaded within the first 24 hours. Following this initial burst, sheet hydrogels released vancomycin gradually over the next 5 days. Ointment hydrogels released only 24.7 ± 1.0% of the total vancomycin loaded within the first 24 hours and continued to release at a similar rate for the next 24 hours. This rapid release period was followed by a more gradual drug release over the following 4 days. As shown in Figure 3A, sheet hydrogels released more of the loaded vancomycin overall as compared to ointment hydrogels (83.6 ± 1.6% versus 67.0 ± 2.6%, respectively) over 6 days. The faster release rate and overall larger vancomycin release from the sheet hydrogels is likely related to the larger swelling of these hydrogels in 1× PBS as compared to the ointment hydrogels. As shown in Figure 2A, the overall increase in mass following incubation of the sheet hydrogels for 48 hours in 1× PBS was nearly 2.4 times greater than this value for the ointment hydrogels. This larger increase in hydration yields an increase in drug releasing area, which is proportional to overall drug release[78].

In both hydrogel types, all of the loaded vancomycin was not released in the 6 day period, despite frequent replacement of the release buffer establishing a vancomycin concentration gradient and driving force for release. We hypothesized that some of the vancomycin release was hindered by molecular interactions between gellan and vancomycin in deionized water (pH ~ 5.5). To probe this hypothesis, we used QCM-D to investigate potential vancomycin-gellan interactions, as shown in

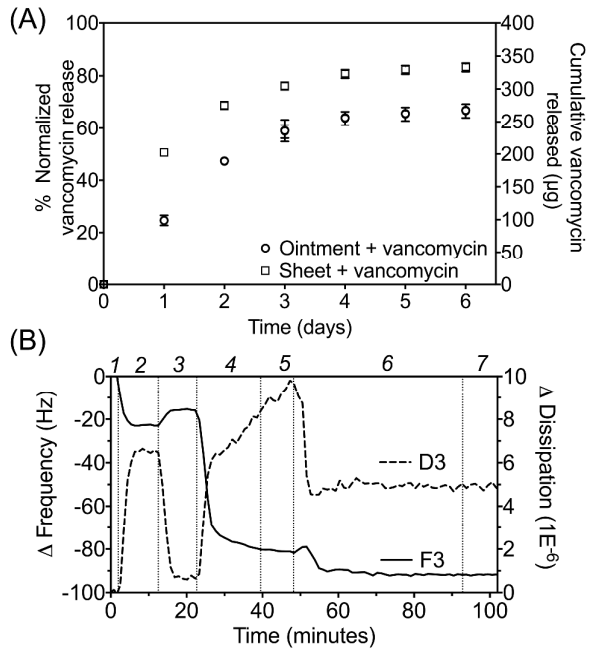

Figure 3: Vancomycin drug release from gellan hydrogels and vancomycin-gellan interaction investigation via QCM-D. (A) Cumulative vancomycin release from vancomycin loaded sheet and ointment hydrogels in 1× PBS at 37°C. Data is shown as a percent cumulative release normalized to the total vancomycin loaded in the hydrogel and an absolute cumulative release (μg) over time. Data are shown as mean ± standard deviation; significance was calculated using two-way ANOVA with Tukey's post-hoc analysis indicating that $p < 0.05$ between subsequent days for cumulative vancomycin release over 6 days (n = 3). (B) QCM-D analysis of vancomycin-gellan interaction; frequency change (ΔF) and dissipation change (ΔD) over time are shown for a representative test (n = 3). Data for the 3rd overtone is shown. Key: 1 = water baseline, 2 = BPEI, 3 = water rinse, 4 = gellan, 5 = water rinse, 6 = vancomycin, 7 = water rinse.

Figure 3B for overtone 3 and Figure S4 for overtones 3, 5, 7, 9, and 11. A layer of BPEI was deposited first to prime the surface with a positively charged polymer in order to promote subsequent adsorption of the polyanionic gellan. A large decrease in frequency was observed following the introduction of gellan (ΔF ~ 60 Hz for overtone 5), along with a large increase in dissipation (corresponding to decreasing rigidity of the surface due to the hydrated polymer interaction). Together the ΔF and ΔD indicate gellan adsorption on the BPEI layer. Following a rinse step, vancomycin was introduced. We observed a decrease in frequency (ΔF ~12 Hz for overtone 5), suggesting vancomycin adsorption, along with a decrease in dissipation. There was no change in the frequency or dissipation values following an extensive rinsing step for over 60 minutes (note: only a portion of this rinse is shown in Figure 3B). The stability in the frequency drop following vancomycin deposition and rinsing indicates favorable molecular interactions between the gellan polymer and vancomycin. Additionally, the decrease in dissipation as compared to the ΔD observed during the gellan adsorption period suggests the formation of interactions between vancomycin and gellan that decrease the viscous nature of the gellan surface prior to vancomycin adsorption (e.g., releasing entrapped water or interacting salts)[56]. Although the exact nature of these interactions was not further investigated, both gellan and vancomycin have an abundance of hydrogen-bonding and electrostatic interaction capabilities that may be involved[79, 80].

In order to understand the vancomycin release mechanism from gellan hydrogels, we applied the Ritger-Peppas[81] and the Peppas-Sahlin models[82], using eqs (6) and (7), respectively. These models can be used to analyze drug release from swellable polymer networks, but have not previously been used to examine drug release mechanisms from such gellan hydrogels.

$$\frac{M_t}{M_\infty} = kt^n \quad (6)$$

$$\frac{M_t}{M_\infty} = k_1 t^m + k_2 t^{2m} \quad (7)$$

Here, M_t is the mass of drug released at time t and M_∞ is the mass of drug released at infinite time. Both semi-empirical models are valid when the fractional drug release $\frac{M_t}{M_\infty} < 0.6$. In the Ritger-Peppas model, k is the kinetic constant and n is the diffusional exponent relating to the mechanism of drug transport; the model is considered applicable when a system does not swell more than 25% of its original volume in drug release conditions[82, 83]. In the Peppas-Sahlin model, k_1 and k_2 are kinetic constants associated with Fickian diffusion and case II relaxation release, respectively; m is the Fickian diffusion exponent, which is a function of the material geometry (m = 0.460 in our case[82]). Case II transport occurs when water penetration into the polymer network is controlled by polymer chain relaxation time[82], affecting drug release rate. Using the Peppas-Sahlin model the contributions to drug release from Fickian diffusion (F) and Case II transport (R) can be compared using eq (8)[82].

$$\frac{R}{F} = \frac{k_2}{k_1} t^m \quad (8)$$

Note that these models were applied only to the sheet hydrogels, as the ointment hydrogels have an amorphous geometry during drug release.

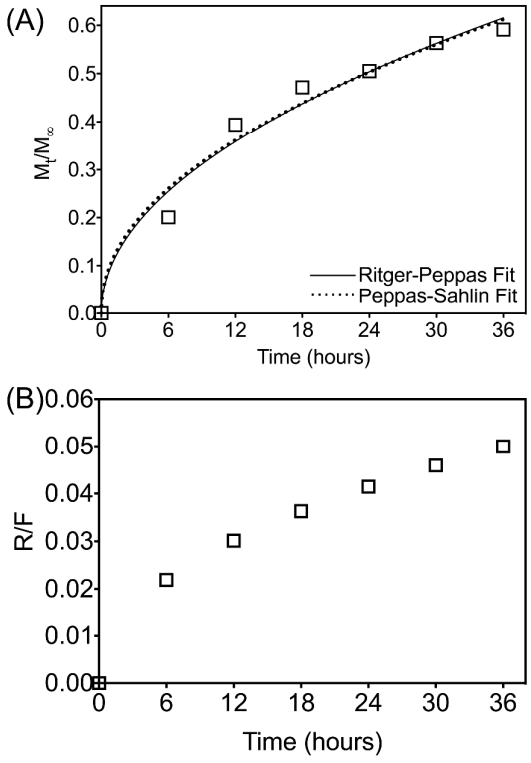

Figure 4: Investigation of drug release mechanism for vancomycin loaded sheet hydrogels. (A) Fractional vancomycin release in 1× PBS at 37°C versus time is shown (where Mt is the mass of drug released at time t and M∞ the mass of drug released at infinite time). Data is given as mean ± standard deviation (n = 3). Best-fit curves for the semi-empirical Ritger-Peppas (R^2 = 0.983) and Peppas-Sahlin (R^2 = 0.982) models are shown. (B) Ratio of Case II relaxation release of vancomycin and Fickian release (R/F) over time for sheet hydrogels, as determined using the Peppas-Sahlin model.

Figure 4A shows vancomycin release data at times satisfying the condition, $\frac{M_t}{M_\infty} < 0.6$ for gellan sheet hydrogels. The best-fit curves obtained using the Ritger-Peppas model and the Peppas-Sahlin model are also shown. Table 2 lists the model outputs obtained from the model fits. The Ritger-Peppas model gives an n value of 0.488. For our cylindrical hydrogels, this n value suggests that vancomycin release from the gellan sheet hydrogels follows an anomalous transport mechanism consisting of both Fickian diffusion and Case II relaxation release. Applying the Peppas-Sahlin model we determined that vancomycin drug release is dominated by Fickian diffusion compared to Case II relaxation ($k_1 >> k_2$), which can be observed in the low R/F

values over time shown in Figure 4B. The increasing R/F value over time does indicate an increased influence of gellan chain relaxation during the drug release incubation period, as we would expect. We also examined how our model outputs changed by assuming that negligible vancomycin release occurs after 6 days, a situation that may occur if vancomycin and gellan interactions indeed hinder additional release, as we have hypothesized. For this scenario, instead of setting the total vancomycin loading in the hydrogel as M_∞ (Scenario 1 in Table 2) we used the 6 day release value (Scenario 2 in Table 2). Doing so, the k_2 value increased by approximately an order of magnitude as shown in Table 2, indicating an order of magnitude greater contribution of Case II relaxation. Regardless of the choice of M_∞, Fickian diffusion dominates vancomycin release from the gellan sheet hydrogels and case II relaxation release also plays a minor role. From the swelling experiments, the uptake of additional liquid by the already hydrated gellan hydrogels, suggests that additional polymer chain relaxation occurs over time in the release conditions contributing to the case II relaxation driven release.

Table 2: Model outputs for vancomycin loaded sheet hydrogel drug release modeling

Model outputs and goodness of fit	Ritger-Peppas		Peppas-Sahlin	
	Scenario 1[a]	Scenario 2[b]	Scenario 1[a]	Scenario 2[b]
k_1	NA	NA	0.112	0.104
k_2	NA	NA	0.001	0.0104
k	0.107	0.101	NA	NA
n	0.488	0.582	NA	NA
$R^{2,c}$	0.983	0.978	0.982	0.975
SSE[c]	0.0060	0.0058	0.0062	0.0064

[a] M_∞ = total vancomycin loading in hydrogel

[b] M_∞ = total vancomycin released by 6 days

[c] R^2 = coefficient of determination; SSE = error sum of squares

Incorporating vancomycin loaded CNPs into gellan hydrogels

After examining vancomycin release from ointment and sheet gellan hydrogel formulations, we were interested in the studying the effects of incorporating vancomycin loaded nanoparticles into these hydrogels. We selected commercially available CNPs to serve as a model nanoparticle for our study. Vancomycin loaded CNPs were incorporated during the hydrogel formation step shown in Figure 1B; the effect of CNP incorporation on mechanical properties and hydrogel gelation, as well as total drug release, drug release timescale, and kinetics was investigated. CNPs are known to adsorb various small molecules due to their high porosity and surface area[52, 84] using weak intermolecular forces[51]. The highly porous CNPs used in this work have a surface area of 150-250 m^2/g and an average diameter of less than 500 nm. We first characterized the vancomycin loading and release capability of these CNPs. Vancomycin and CNPs were mixed in deionized water at a 2:1 w/w ratio; within 10 minutes, more than 85% of the drug available was encapsulated in the CNPs. After 3 hours, we noted that 95% of the available drug had been encapsulated (Figure S6A). In simulated physiologic conditions (1× PBS at 37 °C), the vancomycin loaded CNPs exhibited release of approximately 10% of the encapsulated vancomycin over 96 hours (Figure S6B).

Composite ointment and sheet hydrogels were formulated to contain both free vancomycin and vancomycin loaded CNPs. These hydrogels contained the same total amount of vancomycin as hydrogels formulated without CNPs (i.e., 33.3% of the vancomycin in each hydrogel was contained in CNPs and the remaining 66.7% was added as free vancomycin; some of this "free" drug may potentially also interact with the CNPs during hydrogel fabrication). The addition of drug containing CNPs did not hinder the gellan gelation process. Figure 5A shows digital images of CNP containing ointment hydrogels extruded from a 25.5 gauge needle and cylindrical sheet hydrogels, showing some agglomeration of the particles. Shear thinning behavior of these gels is outlined in Figure S2 as well. SEM images are also shown for these formulations, and look similar to the hydrogels formulated without CNPs. Figure 5B shows the G' and G'' values obtained versus frequency for CNP containing composite hydrogels. As with the non-CNP loaded hydrogels, G' and G'' for the sheet composite hydrogels were approximately 3 orders of magnitude greater than G' and G'' for the ointment composites. We observed no significant difference between G' and G" measurements for hydrogels formulated with and without CNPs (Figure S7). However, we did observe that addition of CNPs caused a stiffening of the sheet hydrogels under compressive load. Compression testing of the sheet composite hydrogels showed an increase in Young's modulus from 135 ± 47 kPa for vancomycin loaded sheet hydrogels to 689 ± 25 kPa for sheet composite hydrogels (Figure S8 shows the stress-strain data for these hydrogels). The CNPs may function similarly to previously reported chemically functionalized nanoparticles that serve as cross-

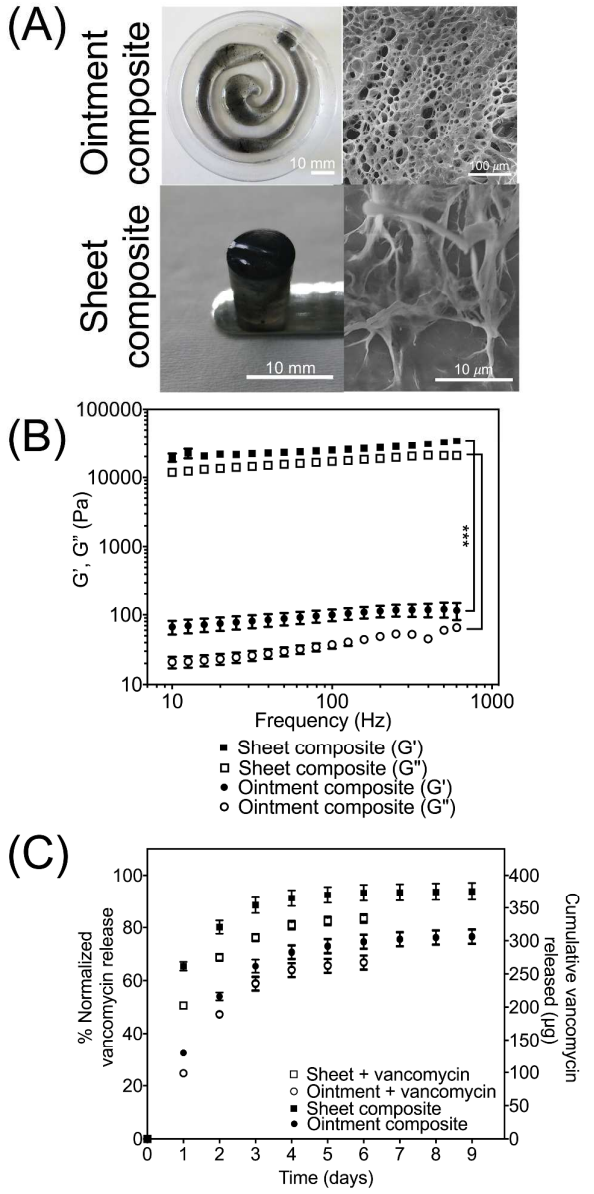

Figure 5: Characterization of composite hydrogels containing free and CNP loaded vancomycin. (A) Representative digital images of composite ointment and sheet hydrogels are shown along with SEM images of freeze-dried and fractured hydrogels. (B) Storage (G') and loss (G") moduli of ointment and sheet composite hydrogels over a frequency sweep of 10 to 600 Hz. Data are shown as mean ± standard deviation; significance was calculated using a two-tailed t-test indicating that ***$p < 0.001$ for G" and G" between sheet and ointment composite hydrogels ($n = 5$). (C) Cumulative vancomycin release from ointment and sheet hydrogels formulated with and without vancomycin loaded CNPs in 1× PBS at 37°C. Data is shown as a percent cumulative release normalized to the total vancomycin loaded in the hydrogel and an absolute cumulative release (μg). Data are shown as mean ± standard deviation; significance was calculated using two-way ANOVA with Tukey's post-hoc analysis indicating that $p < 0.05$ between subsequent days for cumulative vancomycin release over 9 days for CNP containing hydrogels ($n = 3$) and 6 days for hydrogels without CNPs ($n = 3$).

linking epicenters[85, 86]; in this case, the CNPs are not specifically functionalized to interact covalently with gellan, but physicochemical interactions may enable changes in the hydrogel network formation upon compression leading to stiffening.

We found that in all cases, the composite hydrogels had a lower swollen minus initial mass difference and lower rehydration ratio in deionized water as compared to the hydrogels formulated without CNPs (Figure 6 A-D). This difference is likely related to the increased stiffness of the composite hydrogels, lowering polymer chain flexibility and relaxation in the presence of the swelling solution. This phenomenon is especially pronounced in the case of water, which has the largest osmotic pressure difference between the hydrogel and the surrounding solution during swelling studies. A lower swollen minus initial mass difference was also observed for composite hydrogels in 7 mM $CaCl_2$ for ointments (Figure 6A) and 1 mM $CaCl_2$ for sheets (Figure 6B) as compared to non-CNP hydrogels. Q_s trends were similar between the sheet and ointment hydrogels fabricated with and without CNPs as shown in Figure S5. However, exact values cannot be compared as readily, as the hydrogel dry mass varies depending on the formulation.

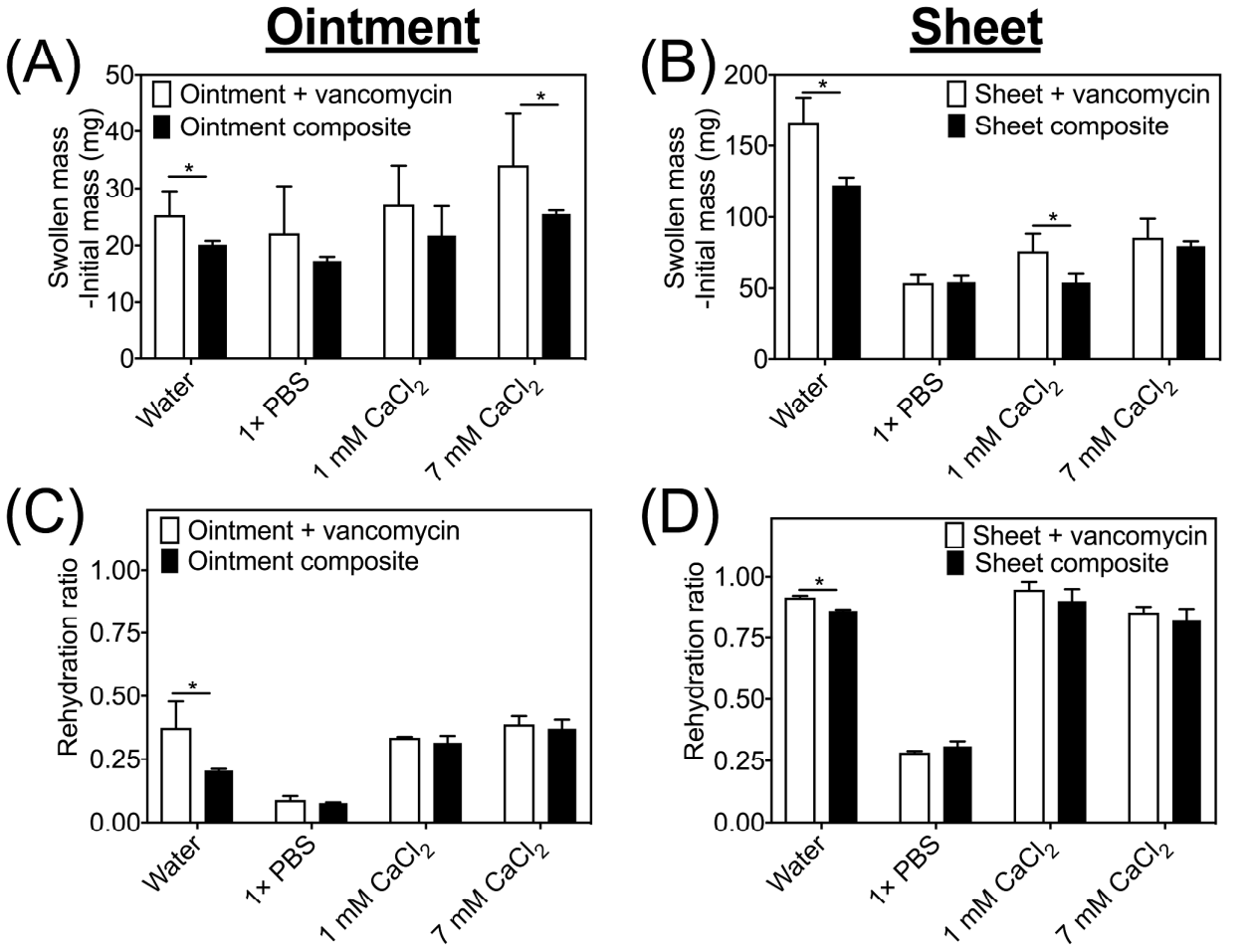

Figure 6: Composite hydrogel swelling analysis in deionized water, 1× PBS, and $CaCl_2$ solutions at 37°C. The mass difference between 48 hour swollen hydrogels and their initial post-hydrogel fabrication mass for (A) ointment hydrogels with and without vancomycin loaded CNPs and (B) sheet hydrogels with and without vancomycin loaded CNPs. Rehydration ratio of hydrogels incubated in the respective swelling solutions following complete dehydration for (C) ointment hydrogels with and without vancomycin loaded CNPs and (D) sheet hydrogels with and without vancomycin loaded CNPs. Data are shown as mean ± standard deviation; significance was calculated using a two-tailed t-test indicating that $*p < 0.05$ between the groups indicated ($n = 3$).

Figure 5C shows a comparison between the vancomycin release from composite hydrogels and hydrogels loaded without CNPs in 1× PBS at 37°C. The CNPs did not leach from the hydrogels during these drug release experiments. We observed that the vancomycin release rate over the initial 24 hours of release for composite hydrogels was 1.3 times that of non-CNP ointment and sheet formulations. Following this period, drug release rates were equivalent between composite and non-CNP hydrogels. The overall vancomycin release time (above MIC and above equipment detection limits of approximately 1 μg/mL) was extended to 9 days as compared to 6 days for hydrogels formulated

without vancomycin loaded CNPs. In this time, sheet composite hydrogels released 93.9 ± 3.3% of the total loaded vancomycin, exceeding the 83.6 ± 1.6% release observed for non-CNP containing sheet hydrogels. Ointment composite hydrogels demonstrated a release of 76.4 ± 2.7% of the encapsulated vancomycin compared with 67.0 ± 2.6% for the non-CNP containing ointment hydrogels. As swelling properties in 1× PBS were similar in both composite and non-CNP hydrogels, the larger initial release of vancomycin from composite hydrogels cannot necessarily be attributed to differences in swelling in these conditions. The large initial release of drug from the CNPs is likely the reason for the initial increase in vancomycin release rate. The overall longer release timeframe of the composite hydrogels relates to the high porosity and tortuosity of the particles containing macro-, micro-, and mesopores[87], leading to additional vancomycin release over time. Interestingly, we also noted that sheet and ointment hydrogels formulated with empty CNPs and the same loading of vancomycin in the hydrogel as hydrogels formulated without CNPs, had a significantly lower release of vancomycin (Figure S9A). We hypothesize that this phenomenon may be a result of vancomycin molecules interacting with the CNPs during the 1× PBS incubation leading to adsorption and entrapment of the drug within the CNPs, hindering release from the gels. This retardation of vancomycin release does not occur with the composite hydrogels as the CNPs appear to already be saturated with vancomycin.

Release of vancomycin from hydrogels containing vancomycin loaded only within CNPs with no free vancomycin within the hydrogel was also observed. The total vancomycin load was kept the same as the other hydrogel formulations examined. For this case, we observed that 42.8 ± 4.7% and 62.1 ± 3.6% of the loaded vancomycin was released from the ointment and sheet hydrogels, respectively, over 9 days (Figure S9B). This release was significantly lower than the release observed from free vancomycin containing hydrogels, both with and without vancomycin loaded CNPs. Free vancomycin is more readily available for release from the hydrogels as compared to the vancomycin that is interacting with the highly porous and tortuous CNPs. The rapid initial release of drug which was observed from the hydrogels lacking free vancomycin can be attributed to the rapid release of drug from the CNPs, which was observed in solution.

We examined hydrogel mass in different conditions as a measure of hydrogel stability. Sheet composite hydrogels and non-CNP loaded hydrogels were stored in 1× PBS or deionized water at 20°C and 37°C over 25 and 77 days, respectively. The percent change in wet mass was determined for samples at various time points over this duration (see Figure S10A and S10B). Negligible mass loss was observed for composite and non-CNP loaded hydrogels stored at 20°C and 37°C in 1× PBS. Non-CNP loaded hydrogels stored in deionized water at 20°C also saw a negligible change in mass over time. At 37°C in deionized water, non-CNP loaded hydrogels experienced a 12.5 ± 5.6% loss in mass compared to 7.37 ± 0.49% for sheet composite hydrogels, indicating enhanced stability of the CNP hydrogels in these conditions. Interestingly, at 7 days in 20°C in deionized water, composite sheet hydrogels experienced a mass loss of 7.22 ± 0.18% as compared to the negligible mass loss observed for non-CNP hydrogels. Overall, the most significant mass change occurred in the first 7 days. The mass loss observed in deionized water may be due to several factors including ion leaching[88] due to concentration differences in water and the hydrogel, and hydrogel network physical disruption due to ion leaching. The impact of these factors may vary with the presence of CNPs. These gellan hydrogels are more stable than other polysaccharide hydrogels including pectin[89] and alginate[24].

Potential clinical applications of vancomycin loaded gellan hydrogels

The gellan hydrogels developed in this work have the potential to be utilized for clinical antimicrobial applications, including wound treatments. Wounds are one of the most common forms of debilitating trauma. If left untreated, bacterial pathogens such as *S. aureus* or MRSA can infect the wounds[42, 90] and may ultimately result in sepsis. Sepsis has a 50% mortality rate leading to 10,000 deaths per year in the United States alone[42, 91]. Hydrogel wound dressings are the current gold standard for treatment of topical wounds, due to their high water content promoting autolytic debridement and high tunability. Many of these dressings do not contain antimicrobial agents, and others that do can exhibit low drug loadings and prolonged release at suboptimal concentrations. Both of these factors can increase bacterial susceptibility to antibiotic resistance[92]. Additionally, many of these dressings must be reapplied daily, leading to further tissue damage and increased treatment costs; the planar design of many can also make them difficult to apply to irregular wound configurations[42]. The vancomycin containing gellan ointment and sheet hydrogels reported in this work offer a potential solution. These hydrogels can be formulated to exhibit a range of mechanical properties, as shown for the ointment and sheet formulations that may be applicable for different wound types. The ointment can be used to fill in irregular wounds, while the sheet hydrogels are appropriate for planar wound configurations. Both options provide vancomycin release over 6 to 9 days at concentrations that are above the MIC against most *S. aureus* and MRSA strains[59, 93, 94], eliminating the need for daily reapplication. Additionally, the large initial vancomycin release can be highly desirable for these applications, allowing for rapid elimination of existing bacteria in the wound[46]. In this work, we examined *in vitro* antimicrobial activity of the hydrogels as well as hydrogel biocompatibility with important wound healing cells, to provide support towards a future use of these materials in wound applications.

The effect of composite sheet and ointment gellan hydrogels against methicillin-susceptible *S. aureus* and a

community-acquired MRSA strain was examined using a modified Kirby-Bauer assay[58]. Figure 7A[95] shows representative results from these studies in which the hydrogel test samples, sheet and ointment gellan hydrogels fabricated without vancomycin, positive controls of commercially available vancomycin loaded discs (30 µg), and negative controls of empty discs were placed on *S. aureus* and MRSA coated agar. As expected, empty sheet and ointment gellan hydrogels behaved similarly to the negative controls, lacking any visible zone of inhibition surrounding the samples for both *S. aureus* and MRSA. For composite sheet and ointment gellan hydrogels, clear zones of inhibition were observed, indicating successful inhibition of both *S. aureus* and MRSA growth. The positive controls also exhibited a zone of inhibition with diameters agreeing with manufacturer reported values for *S. aureus* and MRSA.

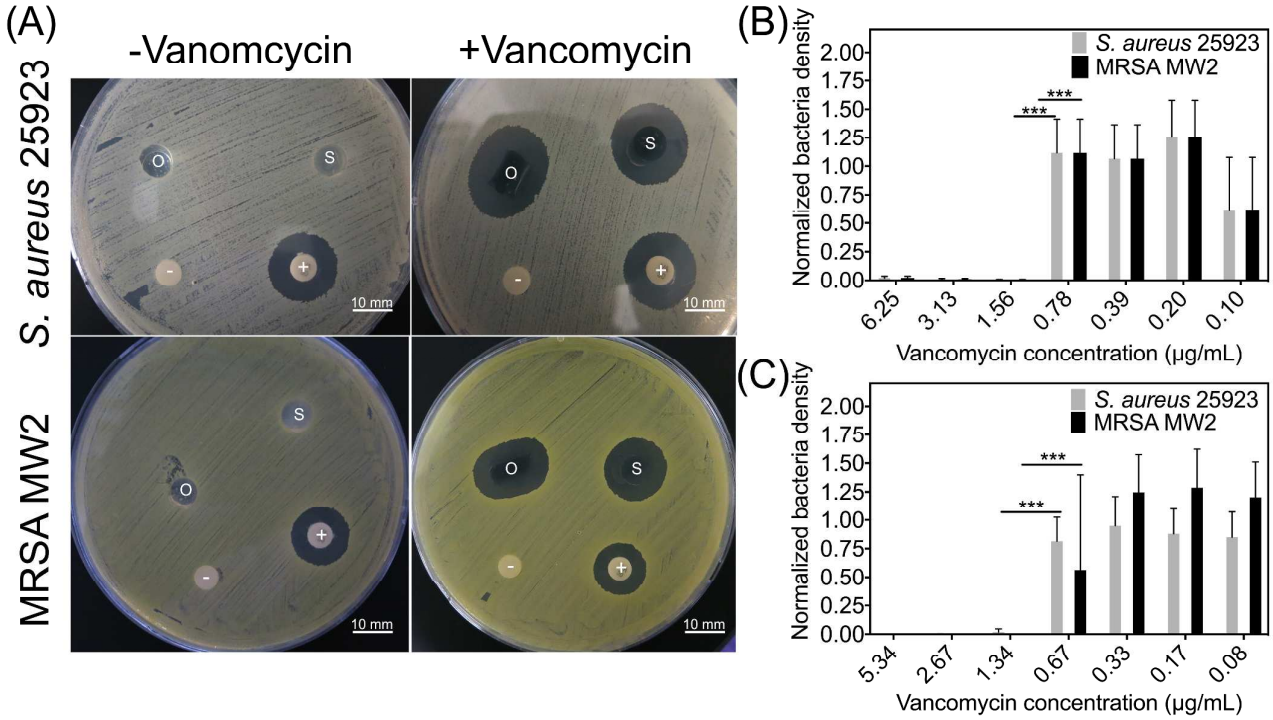

Figure 7: Bacterial growth inhibition in the presence of gellan hydrogels. (A) Representative images of a modified Kirby-Bauer assay show that non-drug loaded hydrogel ointment and sheet controls do not inhibit *S. aureus* or MRSA growth, while composite ointment and sheet hydrogels containing vancomycin are surrounded by clear zones of inhibition against both bacteria. Key: O = ointment; S = sheet; - = blank disc negative control; + = 30 µg vancomycin disc positive control. Normalized *S. aureus* and MRSA density versus vancomycin concentration for dilutions of (B) non-hydrogel incorporated vancomycin standards and (C) vancomycin released from sheet composite hydrogels incubated in 1× PBS at 37°C for 14 days. The vancomycin MIC against both bacteria for hydrogel incorporated drug is unchanged from non-hydrogel incorporated drug. Data are shown as mean ± standard deviation; significance was calculated using a two-tailed t-test indicating that ***$p < 0.001$ for normalized bacteria density between subsequent vancomycin concentrations as indicated ($n = 3$).

We also tested the MIC of vancomycin released from the gellan sheet composite hydrogels against *S. aureus* and MRSA. Figure 7B[95] shows the normalized bacteria density for these strains exposed to non-hydrogel incorporated vancomycin dilutions prepared in 1× PBS, suggesting an MIC in the range of 0.78 – 1.56 µg/mL, which is in agreement with the known MIC of vancomycin against most *S. aureus* and MRSA strains. Figure 7C shows the normalized bacteria density of *S. aureus* and MRSA exposed to dilutions of a 1× PBS solution in which composite sheet gellan hydrogels were incubated at 37°C for 14 days. The MIC of hydrogel-released vancomycin was unchanged compared to the non-hydrogel incorporated vancomycin (Figure 7B), indicating no loss in vancomycin activity. Vancomycin is known to undergo degradation through asparagine deamidation[96] and loss in vancomycin activity has been observed in aqueous formulations[97]. Degradation has been observed in solutions kept at 37°C for only 7 days[98]. It has previously been observed that vancomycin stability can be maintained when it is incorporated into self-assembled multilayer films based on molecular interactions with various polymers[99] and stored in dry conditions. It is possible that the gellan-vancomycin interaction that we observed via QCM-D and potentially vancomycin interaction with the CNPs may stabilize the vancomycin molecule, helping preserve vancomycin activity despite being exposed to a highly hydrated environment (both in the hydrogel and the release buffer) at 37°C for 14 days.

Journal of Materials Chemistry B

ARTICLE

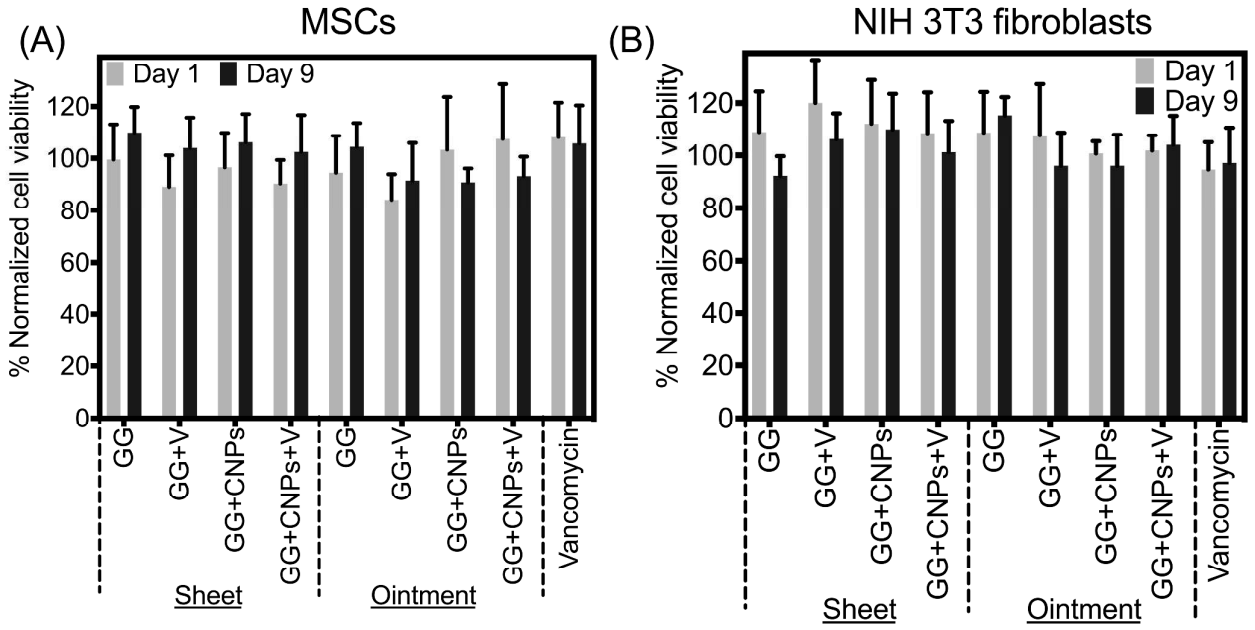

Figure 8: MSC and fibroblast viability for gellan hydrogels. Viability of (A) MSCs and (B) NIH 3T3 fibroblasts in media incubated with hydrogels or a vancomycin control (400 μg) for 1 and 9 days. Sheet and ointment hydrogels with and without free vancomycin were tested, along with sheet and ointment hydrogels containing vancomycin loaded CNPs and empty CNPs. Key: GG = gellan gum hydrogel; V = vancomycin; CNPs = graphitized carbon blank nanoparticles. There was no statistical difference in viability between untreated cell controls and hydrogel or vancomycin treated samples ($p > 0.05$; two-way ANOVA; n = 3).

We also examined *in vitro* viability of fibroblasts and MSCs, common wound healing cells, in the presence of hydrogel incubated media (for 1 and 9 days) and a non-hydrogel incorporated vancomycin control (400 μg). Normalized cell viability was found to be unaffected compared with non-hydrogel exposed media controls for all conditions examined for both cell types (Figure 8). These results lend support for future translation of the hydrogel materials developed in this work.

Conclusions

In this work, we have developed highly tunable, antibacterial hydrogels using gellan gum, $CaCl_2$, vancomycin, and vancomycin loaded CNPs. We have presented a thorough analysis of hydrogel mechanical, swelling, and drug release properties. Overall, we determined that Fickian diffusion dominates vancomycin release from sheet gellan hydrogels, while case II relaxationa release also has a small contribution. Sheet hydrogels release a greater amount of the total loaded vancomycin than ointment hydrogels (83.6 ± 1.6% versus 67.0 ± 2.6%, respectively), which we attributed to the greater swelling of sheet hydrogels in the release buffer as compared to ointment hydrogels. We hypothesize that complete vancomycin release from these hydrogels is inhibited by intermolecular interactions between gellan and vancomycin, which we demonstrated using QCM-D. Therapeutically effective concentrations of vancomycin were released over 6 to 9 days for non-CNP and composite hydrogels, respectively. Our *in vitro* studies demonstrated no loss in hydrogel-released vancomycin activity against *S. aureus* and MRSA and biocompatibility against MSCs and NIH 3T3 cells, supporting the potential use of these hydrogels in the prevention and treatment of wound infections without disrupting wound healing process. Gellan is a unique biopolymer that has only recently gained popularity in application areas beyond food science, including biomaterials development. This work demonstrates that gellan hydrogel composition can be controlled to yield varying drug release properties. The findings of this study may be applied in future development of gellan hydrogels for drug delivery.

Conflicts of Interest

There are no conflicts to declare.

Acknowledgements

We acknowledge support from the Brown University Dean's Emerging Areas of New Science Award and the Office of Naval Research (Award No. N00014-14-1-0798). We thank Tinotenda Gwisai for her assistance in drug release studies and Dr. Alessia Battigelli at Brown for her assistance in mammalian cell cytotoxicity experiments. We would also like to thank Professor Anubhav Tripathi at Brown University for use of the TA Instruments AR2000 rheometer and Professor Braden Fleming at Brown University for use of his Bose Enduratec® ELF 3200. Additionally, we acknowledge the use of the Brown University Institute for Molecular and Nanoscale Innovation's Electron Microscopy Facility and assistance of Anthony McCormick.

Abbreviations

Graphitized carbon black nanoparticles, CNPs; scanning electron microscopy, SEM; phosphate buffered saline, PBS, quartz crystal microbalance with dissipation, QCM-D; methicillin-resistant *Staphylococcus aureus*, MRSA; mesenchymal stem cells, MSCs; Dulbecco's Modified Eagle's Medium, DMEM.

References

1. A. Childs, H. Li, D. M. Lewittes, B. Dong, W. Liu, X. Shu, C. Sun and H. F. Zhang, *Sci Rep*, 2016, **6**, 34905.
2. B. Balakrishnan, M. Mohanty, P. R. Umashankar and A. Jayakrishnan, *Biomaterials*, 2005, **26**, 6335-6342.
3. J. S. Boateng, K. H. Matthews, H. N. Stevens and G. M. Eccleston, *J Pharm Sci*, 2008, **97**, 2892-2923.
4. H. T. Hsieh, H. M. Chang, W. J. Lin, Y. T. Hsu and F. D. Mai, *Sci Rep*, 2017, **7**, 9531.
5. X. Zhao, H. Wu, B. Guo, R. Dong, Y. Qiu and P. X. Ma, *Biomaterials*, 2017, **122**, 34-47.
6. W. Xu, Q. Song, J.-F. Xu, M. J. Serpe and X. Zhang, *ACS Applied Materials & Interfaces*, 2017, **9**, 11368-11372.
7. N. S., K. M. and H. Z. M., *Journal of Applied Polymer Science*, 2018, **135**, 46311.
8. R. Dimatteo, N. J. Darling and T. Segura, *Advanced Drug Delivery Reviews*, 2018, **127**, 167-184.
9. H. Hamedi, S. Moradi, S. M. Hudson and A. E. Tonelli, *Carbohydrate Polymers*, 2018, **199**, 445-460.
10. K. Lee, E. A. Silva and D. J. Mooney, *J R Soc Interface*, 2011, **8**, 153-170.
11. P. Tayalia and D. J. Mooney, *Adv Mater*, 2009, **21**, 3269-3285.
12. S. J. Bryant, R. J. Bender, K. L. Durand and K. S. Anseth, *Biotechnol Bioeng*, 2004, **86**, 747-755.
13. M. J. Mahoney and K. S. Anseth, *Biomaterials*, 2006, **27**, 2265-2274.
14. D. S. Benoit, M. P. Schwartz, A. R. Durney and K. S. Anseth, *Nat Mater*, 2008, **7**, 816-823.
15. D. R. Griffin, W. M. Weaver, P. O. Scumpia, D. Di Carlo and T. Segura, *Nat Mater*, 2015, **14**, 737-744.
16. I. A. Alsarra, *Int J Biol Macromol*, 2009, **45**, 16-21.
17. A. J. DeFail, C. R. Chu, N. Izzo and K. G. Marra, *Biomaterials*, 2006, **27**, 1579-1585.
18. X. Zhu, A. F. Radovic-Moreno, J. Wu, R. Langer and J. Shi, *Nano Today*, 2014, **9**, 478-498.
19. M. McKenna, *Nature*, 2013, **499**, 394-396.
20. A. Shukla, R. C. Fuller and P. T. Hammond, *J Control Release*, 2011, **155**, 159-166.
21. S. Li, S. Dong, W. Xu, S. Tu, L. Yan, C. Zhao, J. Ding and X. Chen, *Adv Sci (Weinh)*, 2018, **5**, 1700527.
22. N. Bhattarai, J. Gunn and M. Zhang, *Adv Drug Deliv Rev*, 2010, **62**, 83-99.
23. S. Dunnhaupt, J. Barthelmes, J. Iqbal, G. Perera, C. C. Thurner, H. Friedl and A. Bernkop-Schnurch, *J Control Release*, 2012, **160**, 477-485.
24. K. Y. Lee and D. J. Mooney, *Prog Polym Sci*, 2012, **37**, 106-126.
25. Q. Zhou, H. Kang, M. Bielec, X. Wu, Q. Cheng, W. Wei and H. Dai, *Carbohydrate Polymers*, 2018, **197**, 292-304.
26. C. Cencetti, D. Bellini, A. Pavesio, D. Senigaglia, C. Passariello, A. Virga and P. Matricardi, *Carbohydr Polym*, 2012, **90**, 1362-1370.
27. W. Yang, E. Fortunati, F. Bertoglio, J. S. Owczarek, G. Bruni, M. Kozanecki, J. M. Kenny, L. Torre, L. Visai and D. Puglia, *Carbohydrate Polymers*, 2018, **181**, 275-284.
28. Z. H. Kang Ding Nishinari Katsuyoshi, *Progress in Chemistry*, 2014, **26**, 1172-1189.
29. E. R. Morris, K. Nishinari and M. Rinaudo, *Food Hydrocolloids*, 2012, **28**, 373-411.
30. M. T. Nickerson, A. T. Paulson and R. A. Speers, *Food Hydrocolloids*, 2003, **17**, 577-583.
31. J. Horinaka, K. Kani, Y. Hori and S. Maeda, *Biophys Chem*, 2004, **111**, 223-227.
32. C. S. F. Picone and R. L. Cunha, *Carbohydrate Polymers*, 2011, **84**, 662-668.
33. D. F. Coutinho, S. V. Sant, H. Shin, J. T. Oliveira, M. E. Gomes, N. M. Neves, A. Khademhosseini and R. L. Reis, *Biomaterials*, 2010, **31**, 7494-7502.
34. C. J. Ferris, K. J. Gilmore, G. G. Wallace and M. I. H. Panhuis, *Soft Matter*, 2013, **9**, 3705-3711.
35. N. A. Silva, M. J. Cooke, R. Y. Tam, N. Sousa, A. J. Salgado, R. L. Reis and M. S. Shoichet, *Biomaterials*, 2012, **33**, 6345-6354.
36. D. R. Pereira, J. Silva-Correia, S. G. Caridade, J. T. Oliveira, R. A. Sousa, A. J. Salgado, J. M. Oliveira, J. F. Mano, N. Sousa and R. L. Reis, *Tissue Eng Part C Methods*, 2011, **17**, 961-972.
37. M. H. Mahdi, B. R. Conway and A. M. Smith, *Int J Pharm*, 2015, **488**, 12-19.
38. P. Matricardi, C. Cencetti, R. Ria, F. Alhaique and T. Coviello, *Molecules*, 2009, **14**, 3376-3391.
39. O. Novac, G. Lisa, L. Profire, C. Tuchilus and M. I. Popa, *Mater Sci Eng C Mater Biol Appl*, 2014, **35**, 291-299.
40. H. M. El-Laithy, D. I. Nesseem, A. A. El-Adly and M. Shoukry, *Archives of Pharmacal Research*, 2011, **34**, 1663-1678.
41. C. Y. Loo, P. M. Young, W. H. Lee, R. Cavaliere, C. B. Whitchurch and R. Rohanizadeh, *Biofouling*, 2014, **30**, 773-788.

42. B. A. Lipsky and C. Hoey, *Clin Infect Dis*, 2009, **49**, 1541-1549.
43. P. V. AshaRani, G. Low Kah Mun, M. P. Hande and S. Valiyaveettil, *ACS Nano*, 2009, **3**, 279-290.
44. B. S. Atiyeh, M. Costagliola, S. N. Hayek and S. A. Dibo, *Burns*, 2007, **33**, 139-148.
45. B. K. Hubbard and C. T. Walsh, *Angew Chem Int Ed Engl*, 2003, **42**, 730-765.
46. A. Shukla, S. N. Avadhany, J. C. Fang and P. T. Hammond, *Small*, 2010, **6**, 2392-2404.
47. A. Shukla, J. C. Fang, S. Puranam and P. T. Hammond, *J Control Release*, 2012, **157**, 64-71.
48. U. Joosten, A. Joist, G. Gosheger, U. Liljenqvist, B. Brandt and C. von Eiff, *Biomaterials*, 2005, **26**, 5251-5258.
49. H. Gu, P. L. Ho, E. Tong, L. Wang and B. Xu, *Nano Letters*, 2003, **3**, 1261-1263.
50. M. Kruk, Z. J. Li, M. Jaroniec and W. R. Betz, *Langmuir*, 1999, **15**, 1435-1441.
51. F. Bruner, G. Crescentini and F. Mangani, *Chromatographia*, 1990, **30**, 565-572.
52. J. Rivera-Utrilla, M. Sanchez-Polo, V. Gomez-Serrano, P. M. Alvarez, M. C. Alvim-Ferraz and J. M. Dias, *J Hazard Mater*, 2011, **187**, 1-23.
53. A. I. Van Den Bulcke, B. Bogdanov, N. De Rooze, E. H. Schacht, M. Cornelissen and H. Berghmans, *Biomacromolecules*, 2000, **1**, 31-38.
54. Y. Hou, A. R. Matthews, A. M. Smitherman, A. S. Bulick, M. S. Hahn, H. Hou, A. Han and M. A. Grunlan, *Biomaterials*, 2008, **29**, 3175-3184.
55. L. Serra, J. Domenech and N. A. Peppas, *Biomaterials*, 2006, **27**, 5440-5451.
56. C. M. Bailey, A. Tripathi and A. Shukla, *Langmuir*, 2017, **33**, 11986-11997.
57. T. Gwisai, N. R. Hollingsworth, S. Cowles, N. Tharmalingam, E. Mylonakis, B. B. Fuchs and A. Shukla, *Biomed Mater*, 2017, **12**, 045010.
58. A. W. Bauer, D. M. Perry and W. M. Kirby, *AMA Arch Intern Med*, 1959, **104**, 208-216.
59. M. D. Appleman and D. M. Citron, *Diagn Microbiol Infect Dis*, 2010, **66**, 441-444.
60. M. Annaka, Y. Ogata and T. Nakahira, *Journal of Physical Chemistry B*, 2000, **104**, 6755-6760.
61. P. S. Rajinikanth and B. Mishra, *Acta Pharm*, 2007, **57**, 413-427.
62. M. Caggioni, P. T. Spicer, D. L. Blair, S. E. Lindberg and D. A. Weitz, *Journal of Rheology*, 2007, **51**, 851-865.
63. C. A. Carmona-Moran, O. Zavgorodnya, A. D. Penman, E. Kharlampieva, S. L. Bridges, Jr., R. W. Hergenrother, J. A. Singh and T. M. Wick, *Int J Pharm*, 2016, **509**, 465-476.
64. J. T. Oliveira, T. C. Santos, L. Martins, R. Picciochi, A. P. Marques, A. G. Castro, N. M. Neves, J. F. Mano and R. L. Reis, *Tissue Eng Part A*, 2010, **16**, 343-353.
65. A. P. Safronov, I. S. Tyukova and G. V. Kurlyandskaya, *Food Hydrocolloids*, 2018, **74**, 108-114.
66. M. Cassanelli, I. Norton and T. Mills, *Food Hydrocolloids*, 2018, **75**, 51-61.
67. S. Agnello, F. S. Palumbo, G. Pitarresi, C. Fiorica and G. Giammona, *Carbohydr Polym*, 2018, **185**, 73-84.
68. A. Bernkop-Schnurch, C. E. Kast and D. Guggi, *J Control Release*, 2003, **93**, 95-103.
69. E. Miyoshi and K. Nishinari, *Colloid and Polymer Science*, 1999, **277**, 727-734.
70. C. Loebel, C. B. Rodell, M. H. Chen and J. A. Burdick, *Nature Protocols*, 2017, **12**, 1521.
71. H. Du, P. Hamilton, M. Reilly and N. Ravi, *Macromol Biosci*, 2012, **12**, 952-961.
72. A. C. Jayasuriya and K. J. Mauch, *Journal of biomedical science and engineering*, 2011, **4**, 383-390.
73. K. Wieczorowska-Tobis, A. Polubinska, A. Breborowicz and D. G. Oreopoulos, *Adv Perit Dial*, 2001, **17**, 42-46.
74. J. E. Elliott, M. Macdonald, J. Nie and C. N. Bowman, *Polymer*, 2004, **45**, 1503-1510.
75. F. Yu, X. Cao, L. Zeng, Q. Zhang and X. Chen, *Carbohydr Polym*, 2013, **97**, 188-195.
76. D. A. De Silva, L. A. Poole-Warren, P. J. Martens and M. in het Panhuis, *Journal of Applied Polymer Science*, 2013, **130**, 3374-3383.
77. F. Horkay, I. Tasaki and P. J. Basser, *Biomacromolecules*, 2000, **1**, 84-90.
78. P. Colombo, P. L. Catellani, N. A. Peppas, L. Maggi and U. Conte, *International Journal of Pharmaceutics*, 1992, **88**, 99-109.
79. R. Chandrasekaran, L. C. Puigjaner, K. L. Joyce and S. Arnott, *Carbohydrate Research*, 1988, **181**, 23-40.
80. B. Xing, C.-W. Yu, K.-H. Chow, P.-L. Ho, D. Fu and B. Xu, *Journal of the American Chemical Society*, 2002, **124**, 14846-14847.
81. P. L. Ritger and N. A. Peppas, *Journal of Controlled Release*, 1987, **5**, 23-36.
82. N. A. Peppas and J. J. Sahlin, *International Journal of Pharmaceutics*, 1989, **57**, 169-172.
83. P. L. Ritger and N. A. Peppas, *Journal of Controlled Release*, 1987, **5**, 37-42.
84. T. R. Rybolt, D. E. Burrell, J. M. Shults and A. K. Kelley, *Journal of Chemical Education*, 1988, **65**, 1009-1010.
85. M. K. Jaiswal, J. R. Xavier, J. K. Carrow, P. Desai, D. Alge and A. K. Gaharwar, *ACS Nano*, 2016, **10**, 246-256.
86. A. C. Balazs, T. Emrick and T. P. Russell, *Science*, 2006, **314**, 1107-1110.
87. G. Newcombe, R. Hayes and M. Drikas, *Colloids and Surfaces A: Physicochemical and Engineering Aspects*, 1993, **78**, 65-71.
88. M. Kunioka and H. J. Choi, *Polymer Degradation and Stability*, 1998, **59**, 33-37.
89. P. A. Markov, N. S. Krachkovsky, E. A. Durnev, E. A. Martinson, S. G. Litvinets and S. V. Popov, *Journal of Biomedical Materials Research Part A*, 2017, **105**, 2572-2581.
90. H. W. Boucher and G. R. Corey, *Clin Infect Dis*, 2008, **46 Suppl 5**, S344-349.
91. E. A. Azzopardi, E. Azzopardi, L. Camilleri, J. Villapalos, D. E. Boyce, P. Dziewulski, W. A. Dickson and I. S. Whitaker, *PLoS One*, 2014, **9**, e95042.
92. J. H. Yang, P. Bhargava, D. McCloskey, N. Mao, B. O. Palsson and J. J. Collins, *Cell Host & Microbe*, **22**, 757-765.e753.
93. M. J. Rybak, E. Hershberger, T. Moldovan and R. G. Grucz, *Antimicrob Agents Chemother*, 2000, **44**, 1062-1066.
94. A. C. A.L. Barry, H. Nadler, L.B. Reller, C.C. Sanders, J.M. Swenson, *Clinical Laboratory Standards Institute*, 1999, **19**, 1-50.

95. *USA Pat.*, 2016.
96. A. S. Antipas, D. G. Vander Velde, S. D. Jois, T. Siahaan and V. J. Stella, *J Pharm Sci*, 2000, **89**, 742-750.
97. L. M. Galanti, J. D. Hecq, D. Vanbeckbergen and J. Jamart, *J Clin Pharm Ther*, 1997, **22**, 353-356.
98. W. M. Mawhinney, C. G. Adair, S. P. Gorman and B. McClurg, *Am J Hosp Pharm*, 1992, **49**, 2956-2959.
99. A. Shukla, S. Puranam and P. T. Hammond, *J Biomater Sci Polym Ed*, 2012, **23**, 1895-1902.

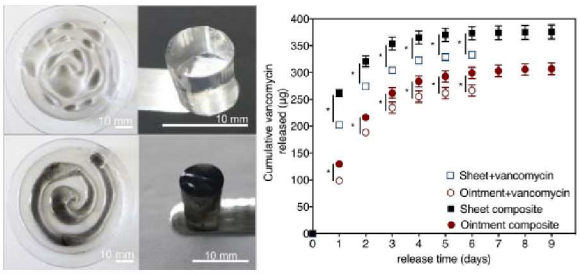

This work highlights the mechanical and drug release tunability of gellan hydrogels containing antibiotics and antibiotic loaded nanoparticles.